Thyroid

DOI: 10.1089/thy.2019.0182

Vps34 PI 3-kinase controls thyroid hormone production by regulating thyroglobulin iodination, lysosomal proteolysis and tissue homeostasis

Giuseppina Grieco[1*], Tongsong Wang[1*], Ophélie Delcorte[1*], Catherine Spourquet[1*], Virginie Janssens[1], Aurélie Strickaert[2], Héloïse P. Gaide Chevronnay[1], Xiao-Hui Liao[3], Benoît Bilanges[4], Samuel Refetoff[3], Bart Vanhaesebroeck[4], Carine Maenhaut[2], Pierre J. Courtoy[1*], and Christophe E. Pierreux[1*#]

[1], Cell Biology Unit, de Duve Institute and Université Catholique de Louvain, 1200 Brussels, Belgium;

[2], Institute of Interdisciplinary Research (IRIBHM); Université Libre de Bruxelles, 1070 Brussels, Belgium;

[3], Departments of Medicine (X-H.L., S.R.) and Pediatrics and Genetics (S.R), The University of Chicago, Chicago, Illinois 60637;

[4], UCL Cancer Institute; University College London, 72 Huntley Street, London WC1E 6DD, UK

[#], correspondence to christophe.pierreux@uclouvain.be

*, equal contributions

Running title: Vps34 controls TH synthesis

Key words: Vps34, thyroid, hormone, organification, autophagy

Dr. Giuseppina Grieco, g.pia@hotmail.it

Dr. Tongsong Wang, tswang0802@hotmail.com

Ms. Ophélie Delcorte, ophelie.delcorte@uclouvain.be

Ms. Catherine Spourquet, catherine.spourquet@uclouvain.be

Ms. Virginie Janssens, virginie.janssens@uclouvain.be

Dr. Aurélie Strickaert, aurelie.strickaert@ulb.ac.be

Dr. Héloïse Gaide-Chevronnay, heloisegaide@hotmail.com

Dr. Xia Hui Liao, xliao1@uchicago.edu

Dr. Benoit Bilanges, b.bilanges@ucl.ac.uk

Prof. Samuel Refetoff, srefetof@uchicago.edu

Prof. Bart Vanhaesebroeck, bart.vanh@ucl.ac.uk

Prof. Carine Maenhaut, cmaenhau@ulb.ac.be

Prof. Pierre J. Courtoy, pierre.courtoy@uclouvain.be

Prof. Christophe E. Pierreux, christophe.pierreux@uclouvain.be

Thyroid

Vps34 PI 3-kinase controls thyroid hormone production by regulating thyroglobulin iodination, lysosomal proteolysis and tissue homeostasis (DOI: 10.1089/thy.2019.0182)

Thyroid
Vps34 PI 3-kinase controls thyroid hormone production by regulating thyroglobulin iodination, lysosomal proteolysis and tissue homeostasis (DOI: 10.1089/thy.2019.0182)
This paper has been peer-reviewed and accepted for publication, but has yet to undergo copyediting and proof correction. The final published version may differ from this proof.

Abstract (327 words, 350 allowed)

BACKGROUND: The production of thyroid hormones (T_3, T_4) depends on the organization of the thyroid in follicles, which are lined by a monolayer of thyrocytes with strict apico-basal polarity. This polarization supports vectorial transport of thyroglobulin for storage into, and recapture from, the colloid. It also allows selective addressing of channels, transporters, ion pumps and enzymes to their appropriate basolateral (NIS, SLC26A7 and Na^+/K^+-ATPase) or apical membrane domain (Anoctamin, SLC26A4, DUOX2, DUOXA2 and TPO). How these actors of T_3/T_4 synthesis reach their final destination remains poorly understood. The PI 3-kinase (PI3K) isoform Vps34/PIK3C3 is now recognized as a main component in the general control of vesicular trafficking and of cell homeostasis via the regulation of endosomal trafficking and autophagy. We recently reported that conditional Vps34 inactivation in proximal tubular cells in the kidney prevents normal addressing of apical membrane proteins and causes abortive macroautophagy.

METHODS: Vps34 was inactivated using a Pax8-driven Cre recombinase system. The impact of Vps34 inactivation in thyrocytes was analyzed by histological, immunolocalization and mRNA expression profiling. Thyroid hormone synthesis was assayed by ^{125}I injection and plasma analysis.

RESULTS: $Vps34^{cKO}$ mice were born at the expected Mendelian ratio and showed normal growth until postnatal day 14, then stopped growing and died at around 1 month of age. We therefore analyzed thyroid $Vps34^{cKO}$ at postnatal day 14. We found that loss of Vps34 in thyrocytes causes: (i) disorganization of thyroid parenchyma, with abnormal thyrocyte and follicular shape and reduced PAS^+ colloidal spaces; (ii) severe non-compensated hypothyroidism with extremely low T_4 levels (0.75 ± 0.62 μg/dL) and huge TSH plasma levels (19,300 ± 10,500 mU/L); (iii) impaired ^{125}I organification at comparable uptake and frequent occurrence of follicles with luminal thyroglobulin but non-detectable T4-bearing thyroglobulin; (iv) intense signal in thyrocytes for the lysosomal membrane marker, LAMP-1, as well as thyroglobulin and the autophagy marker, p62, indicating defective lysosomal proteolysis, and (v) presence of macrophages in the colloidal space.

CONCLUSIONS: We conclude that Vps34 is crucial for thyroid hormonogenesis, at least by controlling epithelial organization, Tg iodination as well as proteolytic T_3/T_4 excision in lysosomes.

Thyroid
Vps34 PI 3-kinase controls thyroid hormone production by regulating thyroglobulin iodination, lysosomal proteolysis and tissue homeostasis (DOI: 10.1089/thy.2019.0182)

Thyroid
Vps34 PI 3-kinase controls thyroid hormone production by regulating thyroglobulin iodination, lysosomal proteolysis and tissue homeostasis (DOI: 10.1089/thy.2019.0182)

Introduction

The main function of the thyroid gland is to produce the hormones, T_4, T_3 , which are essential for the regulation of metabolic processes, and calcitonin (1,2). The production of T_3 and T_4 depends on the correct tissue organization of thyroid epithelial cells, the thyrocytes, into functional and independent units, the follicles. These are composed of a single layer of polarized thyrocytes that form a spherical structure delineating an internal space or lumen where the thyrocyte secretory product, thyroglobulin, is stored in a colloidal form, thus called the colloid lumen. As thyrocytes communicate via gap junctions, each follicle functions as an integrated unit. Thyroid hormone synthesis depends on apico-basal cell polarity that allows the specific localization of channels, transporters, pumps and enzymes at the appropriate membrane domains. Iodide from the bloodstream freely traverses the fenestrated endothelium of the thyroid capillaries and is taken up into thyrocytes via the basolaterally-localized Na^+/I^- symporter (NIS), thanks to a Na^+ gradient generated by the Na^+/K^+-ATPase. An alternative basolateral transporter, SLC26A7, has been recently reported to also control iodide uptake, although its role might be indirect (3). Iodide diffuses freely within thyrocytes and is next transported across the apical membrane into the colloid space via apically-localized transporters such as anoctamin or pendrin (SLC26A4). Iodide is then rapidly oxidized into iodine by thyroperoxidase (TPO) located at the apical membrane, in the presence of H_2O_2, generated by the DUOX2/DUOXA2 apical membrane complex. Iodine is incorporated into accessible tyrosine residues, many of them close to the N- and C-termini of thyroglobulin (Tg), a large protein secreted by thyrocytes into the colloid space. Iodotyrosine rearranges into hormonogenic peptides, which are the direct T_3 and T_4 precursors. Thyroid hormone synthesis thus requires basal localization of NIS, SLC26A7 and Na^+/K^+-ATPase, apical localization of anoctamin, pendrin, TPO, DUOX2 and DUOXA2, as well as apical delivery of Tg into the colloid lumen and endocytic uptake of iodoTg into thyrocyte lysosomes (1,2). Specific regulators of thyroid follicular organization have recently been identified (4). Transcriptomic comparison of thyroid FRT cells cultured in 2D monolayers and in 3D spherical follicles indeed revealed involvement of structural and functional cell elements such as adherens and tight junctions (cadherin-16), cytoskeleton proteins, ions channels,

proteins involved in differentiation, and components of the trafficking machinery (e.g. myosin-Vb, Rab17) (4).

There is strong evidence that vesicular trafficking is critical for apico-basal polarization and epithelial function (5-7), but the role of vesicular trafficking in thyroid function is incompletely understood. Vps34/*PIK3C3* (also referred to as type III PI3K) has long been recognized as a main actor involved in the general control of endocytic vesicular trafficking (8-13). Vps34/PIK3C3 also plays an important role in epithelial organization in *Drosophila* (14) and in autophagy (12,15), both in the initiation of autophagosome formation and the progression towards autophagosome-lysosome fusion (16,17).

We recently inactivated Vps34 in kidney proximal tubular cells using Wnt4-Cre and Pax8-Cre (18,19). Wnt4-Cre driven Vps34 excision caused major perinatal lethality, with abnormalities in kidney cortex development and proximal tubular cell apical differentiation in the surviving mice. With the Pax8-Cre, which triggers recombination in nephrogenic tubules and in nonvascular components of glomeruli two days later than Wnt4-Cre (20,21), we observed normal mouse growth until postnatal (P) day 14 (19). Then, body weight levelled off and all pups died at ~3-5 weeks of age, probably due to kidney failure. Structural and functional studies of $Vps34^{cKO}$ kidneys revealed preserved proximal tubular cell membrane polarity, but impaired apical membrane protein trafficking, thus causing a general proximal tubular cell dysfunction known as renal Fanconi-like syndrome, manifested by polyuria and low-molecular weight proteinuria. $Vps34^{cKO}$ also displayed impaired lysosome size/positioning and blocked autophagy, thereby causing cell vacuolization. We concluded that Vps34 is a crucial component of the trafficking machinery necessary for differentiated proximal tubular cell function and is essential for their overall homeostasis (19). Given that Pax8-Cre also triggers recombination in thyrocytes (21), we here investigated the role of Vps34/PIK3C3 in thyroid function and homeostasis.

Thyroid
Vps34 PI 3-kinase controls thyroid hormone production by regulating thyroglobulin iodination, lysosomal proteolysis and tissue homeostasis (DOI: 10.1089/thy.2019.0182)
This paper has been peer-reviewed and accepted for publication, but has yet to undergo copyediting and proof correction. The final published version may differ from this proof.

Thyroid
Vps34 PI 3-kinase controls thyroid hormone production by regulating thyroglobulin iodination, lysosomal proteolysis and tissue homeostasis (DOI: 10.1089/thy.2019.0182)
This paper has been peer-reviewed and accepted for publication, but has yet to undergo copyediting and proof correction. The final published version may differ from this proof.

Materials and methods

Mice

Vps34$^{fl/fl}$ mice have been described (22). Pax8-Cre mice were obtained from Dr. M. Busslinger (21). Vps34$^{fl/fl}$ mice were crossed with Pax8-Cre;Vps34$^{fl/+}$ mice to generate conditional targeted excision of Vps34 exon 21 in the thyroid of 25% of offspring (Vps34^{cKO}). All the other mice (Vps34$^{fl/+}$, Vps34$^{fl/fl}$ and Pax8-Cre;Vps34$^{fl/+}$) were considered as controls as no differences were observed between these groups. Mice were treated according to the NIH Guide for Care and Use of Laboratory Animals, and experiments were approved by the University Animal Welfare Committee, Université Catholique de Louvain (2016/UCL/MD/006 and 2018/UCL/MD/026).

Plasma, tissue collection and histology

Blood was collected by eye sinus puncture at sacrifice (P14) under irreversible anesthesia by xylazine 2% and ketamine 50 mg/ml (200 µl/mice i.p.). Thyroid lobes were excised, fixed by immersion in neutral-buffered formaldehyde (4% F) at 4°C under stirring overnight. Samples were paraffin-embedded or equilibrated overnight in 20% sucrose and embedded in Tissue-Tek Optimal Cutting Medium (Sakura Finetek) for cryostat sections.

TSH and T4 plasma concentrations

Plasma TSH concentrations were measured by a sensitive, heterologous, disequilibrium double-antibody precipitation RIA as described (23). T4 concentration was measured by coated-tube RIA (Siemens Medical Solution Diagnostics, Los Angeles, CA).

Immunofluorescence

Immunofluorescence was performed on 5 µm-thick frozen sections or on 6 µm-thick paraffin sections (19). Antigen retrieval was promoted in citrate buffer, pH 6.0, at 98°C for 20 min using a Lab Vision Pretreatment Module™ (Thermo Scientific). After permeabilization with PBS/0.3% Triton-X100 for 5 min, non-specific sites were blocked by 1-h incubation in PBS/0.3% Triton-X100 with 10% bovine serum albumin (BSA) and 3% milk, followed by primary antibodies (described in Supplementary Table I) in blocking buffer at 4°C overnight. After extensive washing, sections were incubated with the

appropriate AlexaFluor-secondary antibodies in 10% BSA/0.3% Triton-X100 at room temperature for 1 h, extensively washed, mounted with Faramount Aqueous Mounting Medium (Dako) and imaged on a spinning disk confocal microscope using a Plan Apochromat 100x/1.4 Oil DIC objective (Cell Observer Spinning Disk; Zeiss). For whole thyroid section recording, images were acquired using Zeiss Pannoramic P250 slide scanner, stitched and analyzed using Case Viewer software.

RT-qPCR

Total RNA was extracted from thyroid lobes using TRIzol Reagent (Thermo Scientific), as described (24). Aliquots of 500 ng RNA were reverse-transcribed by M-MLV reverse transcriptase (Invitrogen) with random hexamers, as described (25). Primer sequences used are described in Supplementary Table II. Real-time qPCR was performed as described (25), in presence of 250 nM of specific primers with Kappa SYBR Fast qPCR Master Mix (Kapa Biosystems) on a CFX96 touch real-time PCR Detection System (Bio-Rad). Data were analyzed using the ΔΔCT method, using the geometric mean of *β-Actin* and *Rpl27* as reference genes (26).

^{125}I uptake and organification

At postnatal day 8 (P8), mothers and litters were fed with an iodine-free diet for 24 h. At P9, pups were injected intraperitoneally with 1 µCi ^{125}I (Perkin Elmer) and left for another 24 h before sacrifice and thyroid dissection. Both lobes were collected in 2 mM methimazole (Sigma) and homogenized with a glass Potter. Total thyroid ^{125}I was measured with an automatic gamma counter "Wizard^{2}" (Perkin Elmer) before protein precipitation using 10% trichloroacetic acid (TCA; Merck). After a single wash in TCA, radioactivity was measured in the protein pellet. Percentage of protein-bound iodide was calculated using the ratio of precipitated cpm/total thyroid cpm (27).

H_2O_2 level measurements

The hydrogen peroxide Assay kit from Abcam (ab102500) was used. At P14, thyroid lobes were collected in ice-cold PBS and homogenized with a glass Potter. Proteins were precipitated with perchloric acid 4 M, and supernatant was neutralized with KCl 3 M and

Thyroid
Vps34 PI 3-kinase controls thyroid hormone production by regulating thyroglobulin iodination, lysosomal proteolysis and tissue homeostasis (DOI: 10.1089/thy.2019.0182)
This paper has been peer-reviewed and accepted for publication, but has yet to undergo copyediting and proof correction. The final published version may differ from this proof.

KCl 1 M until pH was comprised between 6.5 and 8. Fifty µl, corresponding to a ninth of a thyroid, was incubated with OxiRed probe and horseradish peroxidase (HRP), according to the instructions form the manufacturer. Fluorescence was measured with a GloMax fluorimeter (Promega, Ex/Em = 535/587 nm).

Statistical analysis

All statistical analyzes were performed with Prism software (GraphPad Software, La Jolla, California, USA). RT-qPCR values were obtained by the ΔΔCT method and are expressed as boxplots with median, 25^{th} and 75^{th} percentiles, and min-max whiskers. Each graph represents the results form a minimum of 8 independent thyroid lobes from at least 3 different litters. Nonparametric statistical tests were used: Mann-Whitney for single comparisons. Differences were considered statistically significant when $p<0.05$ (*); ** stands for $p<0.01$; *** for $p<0.001$.

Results

Genetic construction and assessment of Vps34 inactivation

Ubiquitous Vps34 inactivation is embryonically lethal, with embryos dying around embryonic day E8.5 (28). To study tissue-specific roles of Vps34 *in vivo,* we used a mouse line which carries a floxed *Vps34* allele ($Vps34^{fl}$) that allows to conditionally delete the loxP-flanked exon 21 of the *Vps34* gene, which encodes a critical sequence of the lipid kinase domain of Vps34 (22). This approach was designed to allow for the expression of a minimally-truncated, catalytically-inactive Vps34 protein. However, upon conditional expression in megakaryocytes, the level of this truncated Vps34 and its obligatory partner, Vps15, were found to be decreased by 80-90% in the megakaryocyte lineage (thrombocytes), indicating instability of the truncated Vps34 protein (22). We will thus hereafter refer to the result of this Vps34 truncation as Vps34 conditional knock-out ($Vps34^{cKO}$).

We crossed homozygous $Vps34^{fl/fl}$ mice with Pax8-Cre;$Vps34^{fl/+}$ mice, which is expected to lead to a tissue-specific (thyroid and kidney) conditional excision of exon 21 from both Vps34 alleles in 25% of the pups, which are further referred to as $Vps34^{cKO}$ mice.

Thyroid
Vps34 PI 3-kinase controls thyroid hormone production by regulating thyroglobulin iodination, lysosomal proteolysis and tissue homeostasis (DOI: 10.1089/thy.2019.0182)

Thyroid
Vps34 PI 3-kinase controls thyroid hormone production by regulating thyroglobulin iodination, lysosomal proteolysis and tissue homeostasis (DOI: 10.1089/thy.2019.0182)

Vps34^{cKO} mice were born at the expected Mendelian ratio and showed normal development until postnatal day 14 (P14), then stopped growing and died at around 1 month of age (19). We therefore analyzed the thyroid of Vps34^{cKO} mice at P14. Of note, eye opening, a marker of cerebral maturation was usually delayed till P10.

We first assessed the extent of Vps34 genetic excision in the thyroid by quantification of *Vps34* mRNA using primers that are specific for the total *Vps34* or are exon 21-specific. Compared to control littermate pups, we found a ~70 % reduction of exon 21-containing *Vps34* mRNA in cKO thyroid extracts. In comparison, we found no significant difference in the abundance of *Vps34* mRNA containing exon 22-24 (Fig. 1A). Assuming that *Vps34* is equally expressed in all thyroid cell types (expressing and non-expressing the Cre recombinase), this ~70 % decrease suggests that most thyrocytes in Vps34^{cKO} mice had undergone Cre-mediated recombination.

Vps34^{cKO} thyroids show signs of hyperstimulation by thyroid stimulating hormone (TSH)

At P14, thyroid glands from Vps34^{cKO} were almost twice as heavy as control glands (Fig. 1B). Histological staining using Periodic-Acid-Schiff (PAS, which in the thyroid reflects production of the thyroglobulin glycoprotein) readily revealed striking differences between thyroid glands of control and Vps34^{cKO} mice (Fig. 1C). Thyroid glands of control mice appeared as assemblies of round follicular sections of variable diameter, filled intensely with colloid and homogenously stained by PAS. Although the histological pattern of Vps34^{cKO} was more variable, three representative individual thyroid sections shown in Fig. 1C illustrate irregular follicle shape, especially at the periphery of the gland, and weaker or absent PAS staining (Fig. 1C and Suppl. Fig. 1). In addition, the PAS-negative follicular spaces were often filled with nuclei (see Vps34^{cKO} #3). Quantification revealed that 90% of control follicles had a regular shape and intense (+++) PAS staining (Suppl. Fig. 1). In contrast, only 50% of Vps34^{cKO} follicles displayed a regular shape and most of the follicles were weakly positive for PAS (++ or +) (Suppl. Fig. 1). In addition, 10 to 50% of the Vps34^{cKO} follicles showed no PAS staining (-) and luminal cells were found in 40-70% of the follicles (Suppl. Fig. 1). Confocal immunofluorescence microscopy for the epithelial marker E-cadherin confirmed heterogeneity of Vps34^{cKO} follicles, but also of thyrocytes. Hoechst

labelling revealed the presence of several nuclei in a significant fraction of lumina (Fig. 1D). These histological features of follicle remodelling and colloid consumption up to exhaustion, suggested perturbed thyroid function.

Vps34^{cKO} causes severe non-compensated hypothyroidism

To directly test the hypothesis that Vps34^{cKO} could impair thyroid hormone production, plasma was collected at P14 and analyzed for the levels of T_4 and TSH. In P14 control pups, values were 6.4 ± 1.5 μg/dL for T_4, and 75 ± 110 mU/L for TSH (Fig. 2). In Vps34^{cKO} mice, we found extremely low T_4 values (0.75 ± 0.62 μg/dL) and very high plasma levels of TSH (19,311 ± 10,482 mU/L) (Fig. 2). These data indicate severe, non-compensated hypothyroidism. This observation, compatible with the growth retardation observed after P15 (19), could be explained by mislocalization of one or several basolateral and/or apical actors involved in thyroid hormone synthesis, as we reported in Vps34^{cKO} kidney proximal tubular cells (19).

Vps34 cKO display reduced iodine organification

The reduced or absent PAS staining (Fig. 1C) and the low T_4 plasma levels in Vps34^{cKO} mice (Fig. 2) might be caused by defective basolateral iodine uptake, apical transport and/or apical organification into thyroglobulin. Due to lack or very poor specificity of antibodies directed against murine proteins involved in these processes, we first measured their mRNA expression levels in total thyroids at P14 (Fig. 3). We observed no change in mRNA expression of *Nis*, *Ano1*, *Tg*, *Tpo* and *Duox2,* a significant increase in *Tshr* and *Slc26a4* expression, and a significant decrease of *Slc26a7* and *Duoxa2* mRNA levels. At this stage, we cannot conclude if these changes contribute to the observed hypothyroidism of Vps34^{cKO}.

To further test whether basolateral NIS and SLC26A7 and apical ANO1, SLC26A4, TPO, DUOX and DUOXA were all correctly localized, we functionally assayed their combined activity by injecting iodine-deprived pups at P9 with ^{125}I. At P10, 24-h post-injection, thyroid lobes were collected and radioactivity measured before and after protein precipitation by TCA (Fig. 4A). ^{125}I uptake was not statistically-different in Vps34^{cKO} as

Thyroid
Vps34 PI 3-kinase controls thyroid hormone production by regulating thyroglobulin iodination, lysosomal proteolysis and tissue homeostasis (DOI: 10.1089/thy.2019.0182)
This paper has been peer-reviewed and accepted for publication, but has yet to undergo copyediting and proof correction. The final published version may differ from this proof.

compared to controls (Fig. 4A), suggesting normal NIS and SLC26A7 function and thus basolateral localization. In marked contrast, only 10% of thyroid ^{125}I was bound to proteins in Vps34^{cKO} compared to approximately 55% in controls at this stage (Fig. 4A). This indicates a major effect of Vps34 on one or several apical proteins involved in iodine organification.

Normal *Ano1* and increased *Slc26a4/Pendrin* mRNA levels suggested correct, or even increased, transfer of iodine in the follicular lumen. On the other hand, decreased *Duoxa2* might impact on H_2O_2 production. We thus measured the production of H_2O_2 in control and Vps34^{cKO} thyroid lobes. Surprisingly, the median level of H_2O_2 production in Vps34^{cKO} was higher, even if we observed variability (Fig. 4B), indicating that the DUOX/DUOXA pair is functional in Vps34^{cKO} thyroid tissue. Altogether, these results suggest defective localization of one or several apical actors involved in iodine organification.

Apical polarity is impaired in Vps34^{cKO}

Apico-basal polarity is essential for thyrocyte function and defects in polarity might impact on the delivery, and thus localization, of actors involved in thyroid hormone synthesis. As general markers to assess polarity, we used the basement membrane protein laminin, the basolateral Na^+/K^+-ATPase, E-cadherin and β-catenin, the apically-localized ERM family member ezrin, and the tight junction-associated protein ZO-1. Control thyrocytes displayed a well-defined apico-basal polarity with laminin assembled on the basal side, with Na^+/K^+-ATPase, E-cadherin and β-catenin restricted to the basolateral membrane and separated from apical ezrin by the tight junction, visualized by ZO-1 (Fig. 5A and 5B). In Vps34^{cKO} thyrocytes, basal laminin was correctly assembled and Na^+/K^+-ATPase, E-cadherin and β-catenin were restricted to the basolateral membrane, indicating the presence of functional tight junctions. However, on the apical side of Vps34^{cKO} thyrocytes, the ezrin signal was weaker or absent from the lumen-facing pole of some thyrocytes (Fig. 5A), and most cells also lacked ZO-1 protein labelling (Fig. 5B). These data suggest impaired apical polarity in Vps34^{cKO}, which might contribute to defective localization of apical actors involved in iodine organification.

Thyroid
Vps34 PI 3-kinase controls thyroid hormone production by regulating thyroglobulin iodination, lysosomal proteolysis and tissue homeostasis (DOI: 10.1089/thy.2019.0182)
This paper has been peer-reviewed and accepted for publication, but has yet to undergo copyediting and proof correction. The final published version may differ from this proof.

Thyroid

Vps34 PI 3-kinase controls thyroid hormone production by regulating thyroglobulin iodination, lysosomal proteolysis and tissue homeostasis (DOI: 10.1089/thy.2019.0182)

Vps34^{cKO} mice display defective thyroglobulin iodination

To further analyze the significance of the lack of PAS staining in a fraction of Vps34^{cKO} follicles (Fig. 1C) and the defect in iodine organification (Fig. 4), we assessed thyroglobulin protein expression and its associated T_4 hormonogenic peptide (I-Tg) by immunofluorescence. Low magnification of control sections showed an identical distribution pattern of thyroglobulin and I-Tg, homogeneously filling all round colloidal spaces (Fig. 6A). In Vps34^{cKO}, the thyroglobulin labelling was more heterogeneous, mainly due to the presence of cells in the colloid. Remarkably, antibodies recognizing the T_4 hormonogenic peptide often failed to label colloidal spaces even when containing Tg in the adjacent section (Fig. 6A), thereby confirming the organification defect (Fig. 4A). Quantifications of 5 control thyroids revealed that 96% of the follicles are positive for I-Tg (2712 follicles counted; Suppl. Fig. 2). In contrast, only a quarter (25.2 ± 11.9 %) of Vps34^{cKO} follicles were positive for the T_4-containing hormonogenic peptide (3436 follicles counted in 7 independent thyroids; Suppl. Fig. 2). Of specific interest, whereas the Tg signal was restricted to the follicle lumen in control thyroid tissue, high magnification revealed that the Tg signal was frequently seen within Vps34^{cKO} thyrocytes (Fig. 6B, arrowheads). These observations indicate that Vps34 deletion is associated with defective thyroglobulin iodination, as well as reduced Tg exocytosis and/or excessive Tg endocytosis.

Impaired lysosomal function and I-Tg proteolysis in Vps34^{cKO} thyroid

Vps34 is involved in endocytic trafficking and cKO of Vps34 in postnatal kidney glomeruli podocytes causes a strong increase of the overall immunofluorescence signal for the lysosomal membrane marker LAMP-1, indicating enhanced lysosome biogenesis (29,30). We further reported that absence of Vps34 in kidney proximal tubular cells causes an increase in the actual size of lysosomes, that were sometimes enlarged, and mislocalized toward the basal pole of the cell (19). Given that lysosomal proteases in thyrocytes are important to excise hormonogenic peptides to release free T_3 and T_4, we investigated LAMP-1-labeled structures in Vps34^{cKO} thyrocytes as a proxy for lysosomal function, and its co-localization with Tg and I-Tg to demonstrate endocytosis. In our conditions, immunofluorescence on control thyroid sections only produced a weak LAMP-

Thyroid
Vps34 PI 3-kinase controls thyroid hormone production by regulating thyroglobulin iodination, lysosomal proteolysis and tissue homeostasis (DOI: 10.1089/thy.2019.0182)

1 signal in the E-cadherin-positive epithelial thyrocytes (Fig. 7A and 7B). On the contrary, a strong and widespread LAMP-1 signal was observed in all Vps34^{cKO} thyrocytes. As shown in the enlarged boxes of Fig. 7A and 7B (separate emission channels in white), LAMP-1-positive late endosomes/lysosomes were more abundant, and sometimes enlarged in Vps34^{cKO} thyrocytes as compared to controls. In addition, the intracellular Tg protein, found in most Vps34^{cKO} thyrocytes (Fig. 7A, arrowheads), most often colocalized with LAMP-1-positive structures. This indicates that colloidal Tg was endocytosed by thyrocytes, but that trafficking to or Tg proteolysis within the lysosomes was slower or impaired, as compared to controls. Of note, luminal cells also contained LAMP-1 structures positive for Tg (Fig. 7A, right).

Additional supporting evidence for impaired lysosomal proteolysis is based on the analysis of I-Tg (Fig. 7B). Indeed, Vps34^{cKO} thyrocytes often contain intracellular signal for I-Tg, colocalizing within LAMP-1 structures (Fig. 7B, enlarged boxes,). Thus, in addition to reduced iodine organification, defective lysosomal proteolysis of T_3/T_4, if/when hormonogenic peptides were still formed on Tg, is also potentially contributing to the low T_3/T_4 plasma levels observed in Vps34^{cKO} mice (Fig. 2).

Evaluation of autophagy in Vps34^{cKO} thyroid

The deletion of Vps34 in the kidney also causes a block of autophagy (19). We therefore assessed the expression of p62 (also called sequestosome-1, or SQSTM1), a polyubiquitin-binding protein that interacts with LC3b (microtubule associated protein 1 light chain) on the autophagosome membrane and is normally continuously degraded by the autophagy process (31). Since p62 accumulates when completion of autophagy is inhibited, p62 can be used as a marker to study autophagic flux (32). Although we found a weak punctiform LC3 signal in control thyrocytes, we observed no p62 signal, indicating normal autophagic flux in control thyroid tissue. As reported, few LAMP-1-labelled structures were found in control thyroids. In contrast, much larger structures, mostly double-labeled for p62 and LC3, were easily detected in the cytoplasm of Vps34^{cKO} thyrocytes. As the LAMP-1 signal was increased in Vps34^{cKO}, these p62/LC3-positive punctae sometimes co-localized with LAMP-1. We conclude that LC3 could be recruited on

p62 aggregates but that progression to autophagosome maturation and fusion with, and degradation by, lysosomes is arrested. This suggests that deletion of Vps34 in thyrocytes abrogates the autophagic flux.

Recent evidence has demonstrated that p62 is also an activator of the antioxidant KEAP1/NRF2 pathway, which impacts on thyrocyte physiology and Tg biology (33). We thus examined the possibility that stabilized p62 would compete with NRF2 for KEAP1 binding in Vps34^{cKO}, thus allowing NRF2 to reach the nucleus and activate gene expression. We quantified the mRNA levels of *Nrf2* and its target genes *Nqo1*, *Gpx2* and *Txnrd1*. Although we measured a slight decrease of *Nrf2* mRNA in Vps34^{cKO}, two of its target genes, namely the quinone reductase, *Nqo1*, and the thioredoxin reductase 1, *Txnrd1*, were upregulated 1.9- and 3.5-fold, respectively (Fig. 8B). This observation supports the hypothesis that KEAP1 interaction with p62 is favored in Vps34^{cKO} and that NRF2 is thus displaced and able to migrate to the nucleus to regulate gene expression.

We also evaluated macroautophagy/mitophagy by immunolocalizing TOM20 and LAMP-1. In Vps34^{cKO} thyrocytes, TOM20-labeled structures did not colocalize with the more abundant, enlarged LAMP-1+ structures (Suppl. Fig. 3A), as we also reported in Vps34^{cKO} kidney proximal tubular cells (19). This suggested that sequestration of mitochondria into autophagosomes is either not triggered, which is unlikely for altered cells, or abortive at P14 in Vps34^{cKO} thyrocytes, and/or that fusion of autophagosomes with lysosomes is prevented. We then evaluated the chaperone-mediated autophagy by immunolocalizing LAMP-2A. As compared to control thyroid, LAMP-2A-labeled structures were more abundant in Vps34^{cKO} thyrocytes (Suppl. Fig. 3B), as we also reported in Vps34^{cKO} kidney proximal tubular cells (19).

Luminal cells present in Vps34^{cKO} follicles are macrophages

Finally, we investigated the origin of the cells present in the colloidal space. As observed in Figure 7A, cells trapped in the follicular lumen showed a strong LAMP-1 signal (Fig. 7A). However, they were negative for E-cadherin (Figs. 1D and 5A). In addition, we found that luminal cells were also negative for the permanently-expressed thyrocyte-restricted transcription factor TTF-1 (NKX2.1) (Fig. 9A), indicating that these cells were not

Thyroid

Vps34 PI 3-kinase controls thyroid hormone production by regulating thyroglobulin iodination, lysosomal proteolysis and tissue homeostasis (DOI: 10.1089/thy.2019.0182)

derived from the thyrocyte lineage. Lineage-tracing experiments on Pax8-Cre; Vps34$^{fl/fl}$;ROSA-STOP-YFP pups at P14 further revealed YFP-positive signal only in follicle-delineating thyrocytes and not in the luminal cells (Fig. 9B). Thus, luminal cells had never expressed Pax8 and are therefore not derived from thyrocyte progenitors. Although infiltration by C-cells is a possibilty, we failed to label luminal cells for the Prox1 transcription factor. As luminal cells displayed LAMP-1 signal and were also positive for Tg (Fig. 7A), we tested the possibility that luminal cells were infiltrating macrophages. This is indeed the case because luminal cells were positive for the macrophage marker F4/80 (Fig. 10A), but not by E-cadherin. To confirm that colloid was consumed by infiltrated macrophages, we performed a triple immunolabelling for F4/80, LAMP-1 and I-Tg. Luminal F4/80-positive cells displayed huge LAMP-1-positive lysosomes filled with I-Tg (Fig. 10B). Thus, colloid consumption (Tg in Fig. 7A and I-Tg in Fig. 9D) by infiltrated macrophages provides a third potential explanation for the low T_4 plasma level observed in Vps34^{cKO}.

Discussion

In this study, we report that deleting Vps34 in thyrocytes by Pax8-Cre-driven recombination causes several defects in the thyroid: (i) doubling of thyroid weight and perturbed thyroid parenchyma organization, with reduced PAS$^+$ colloidal spaces; (ii) severe hypothyroidism with collapsed plasma T_4 levels and very high TSH; (iii) a strong decrease of ^{125}I organification, at comparable ^{125}I uptake, and of T_4 formation on thyroglobulin (detected by immunofluorescence as early as P3); (iv) defective apical polarization; (v) impaired lysosomal proteolysis; and (vi) infiltration of macrophages in the colloid. Some of these features, combined with delayed “eye opening” and impaired postnatal growth after two weeks (18), phenocopy the impact of the *Duoxa2* KO in the thyroid (34).

DUOXA2 is a chaperone protein required for the correct localization of DUOX2 at the apical pole of thyrocytes, where the complex (DUOX2/DUOXA2) produces H_2O_2. In the absence of DUOXA2, H_2O_2 is not produced and subsequent thyroperoxidase-mediated oxidation of iodide into reactive compounds and thyroglobulin iodination are abolished (34). The similarity of the severity of hypothyroidism in Vps34^{cKO} and *Duoxa2* KO mice prompted us to have a closer look at DUOXA2 in Vps34^{cKO}. We found that the expression of

Duoxa2 started decreasing after P3, reaching two-fold lower values at P14. It is interesting to note that expression of *Duox2* and *Duoxa2* mRNAs was quantitatively different, despite of the fact that they share the same promoter (35). Whether decreased *Duoxa2* mRNA expression is reflected by an equivalent two-fold decrease of DUOX2/DUOXA2 complex at the apical pole is unknown. However, it is very unlikely that a two-fold decrease would by itself thyroglobulin iodination to such a severe extent, since heterozygous mice for *Duoxa2* deletion have virtually no phenotype. In addition, our measurements of H_2O_2 levels in total Vps34^{cKO} thyroid extracts also support normal, or increased, function of the DUOX2/DUOXA2 complex. Instead, based on the known functions of Vps34 in kidney proximal tubular cells, where its inactivation causes lack of apical localization of endocytic receptors (megalin, cubilin) and solute transporters (NaPi-IIa, SGLT-2) (19), it would be extremely interesting to localize actors of thyroid hormonogenesis on thyroid sections, and assess their basolateral or apical addressing in Vps34^{cKO} thyrocytes. Unfortunately, reliable antibodies to detect most of these proteins are not yet available for mice. Nevertheless, ^{125}I uptake and processing experiments suggest normal localization and function of the sodium-iodine symporter, NIS, and/or the putative alternative transporter SLC26A7 (3), and rather support the hypothesis of defective apical localization of one or several actors involved in thyroid hormonogenesis (Ano1, pendrin (SLC26A4), TPO, DUOX, DUOXA).

Characteristic histopathological alterations combined with the very high plasma TSH levels and a two-fold increase in *Tshr* expression in Vps34^{cKO} thyroid suggest that thyrocytes are in a hyperstimulated state. For example, DuoxA2 KO mice, which display very high TSH levels, present a 20- and 5-fold higher expression level of *Nis* and *Tpo*, as compared to controls (34). However, the expression of these two sensitive target genes of the TSH signaling pathway, *Nis* and *Tpo*, was surprisingly unchanged in Vps34^{cKO} mice, thus arguing against thyrocyte hyperstimulation. We favor the hypothesis of TSHR mistrafficking into intracellular vesicles. Recent work in *Drosophila* revealed that Vps34 inactivation or pharmacological inhibition using the small molecule inhibitor SAR405 causes alteration of cell polarity and disruption of epithelial architecture by relieving LKB1 inhibition and triggering JNK activation (14). A role of Vps34 in epithelial organization and polarity was also observed in 3D cultures of Caco-2 kidney cells (14). It would be interesting to analyze

the activation states of LKB1 and JNK in Vps34^{cKO} thyroid tissue, and, if modified, to cross Vps34^{cKO} with floxed LKB1 alleles.

The expression patterns of the two SLC transporters, *Slc26a7* and *Slc26a4*, in Vps34^{cKO} mice are surprising. The decreased expression of Slc26a7 (4-fold) in Vps34^{cKO} may affect entry of iodine in the thyroid. However, it should be mentioned that this alternative basolateral transporter, SLC26A7, may only play an indirect role on iodine uptake (3). In addition, expression of the main transporter, *Nis*, is at least 16-fold more important than that of *Slc26a7*. This may explain why ^{125}I uptake is not affected. Expression of the apical *Slc26a4* (pendrin) in Vps34^{cKO} was even more dramatic with a 20-fold increase in expression. However, we do not think that this would have affected apical transport of iodine. Indeed, in control thyroids, the expression levels of *Slc26a4* were 60-fold lower than those of *anoctamin1* (6 Ct). This suggests a more prominent role for *anoctamin1* in apical iodide transport (36). These changes in expression of *Slc26a7* and *Slc26a4* could however impact on thyrocyte ion balance. Indeed, SLC26A7 and SLC26A4 transporters have opposite action on chloride ions at the basolateral and apical membranes, respectively. Decreased levels of SLC26A7 at the basolateral membrane may decrease the export of chloride out of the thyrocyte (3). On the contrary the increase of SLC26A4 at the apical membrane may increase the entry of chloride in the thyrocyte. Accumulation of chloride may in turn decrease intracellular pH and causes cellular stress in Vps34^{cKO}.

The weak PAS staining in Vps34^{cKO} could be due to decreased exocytosis of Tg or increased Tg endocytosis. We frequently observed intracellular Tg in Vps34^{cKO} mice. We suggest that the defective process is the endocytic route rather than exocytosis because we readily observed intracellular structures positive for iodinated Tg. This is rarely the case in control thyrocytes where I-Tg is rapidly proteolytically processed. In addition, our work also demonstrates increased abundance and size of LAMP-1-positive late endosomes/lysosomes in Vps34^{cKO} thyrocytes, with accumulation of Tg and the autophagic marker p62, which is indicative of a defective lysosomal trafficking and/or function. In addition to impaired Tg iodination, low T_4 plasma levels thus presumably also result from impaired endocytic transport of I-Tg to lysosomes and/or proteolytic excision of T_3/T_4 therein. Several studies have reported a role for Vps34 in endocytic trafficking to lysosomes

Thyroid
Vps34 PI 3-kinase controls thyroid hormone production by regulating thyroglobulin iodination, lysosomal proteolysis and tissue homeostasis (DOI: 10.1089/thy.2019.0182)
This paper has been peer-reviewed and accepted for publication, but has yet to undergo copyediting and proof correction. The final published version may differ from this proof.

Thyroid
Vps34 PI 3-kinase controls thyroid hormone production by regulating thyroglobulin iodination, lysosomal proteolysis and tissue homeostasis (DOI: 10.1089/thy.2019.0182)
This paper has been peer-reviewed and accepted for publication, but has yet to undergo copyediting and proof correction. The final published version may differ from this proof.

(13, 15, 30, 37) and activation of lysosomal proteases (15). In our study on Vps34^{cKO} renal proximal tubular cells, we also observed an enlargement of lysosomes and their filling by undigested material, labelled for a variety of antigens (19). In Vps34^{cKO} thyrocytes, we also observed an increased abundance and size of LAMP-1-positive compartments filled with Tg and I-Tg. Based on these and previous findings showing that Vps34 deletion leads to late endosome/lysosome enlargement and defective lysosomal function (37), we assume a defective proteolytic excision of T_3/T_4 from I-Tg, analogous to what we reported in cystinotic *Ctns*$^{-/-}$ mice (38). Cystinosis is a lysosomal storage disease caused by deletion or inactivating mutations of the lysosomal cystine transporter cystinosin (39). Defective cystinosin impacts on lysosomal proteolysis, presumably due to endolysosomal mislocalization, impaired pro-cathepsin maturation and altered luminal redox status; moreover, autophagic flux is also altered (40). Like cystinotic patients, *Ctns*$^{-/-}$ mice show compensated hypothyroidism with moderate increase of TSH, thyrocyte hyperplasia and proliferation, combined with progressive colloid depletion and evidence of increased endocytosis into colloid droplets. Iodo-thyroglobulin could be detected in *Ctns*$^{-/-}$ but not wild-type thyrocyte lysosomes, under identical labelling conditions, further indicating defective proteolysis. Continue here

It has recently become clear that Vps34 may act on lysosome positioning, which is crucial to autophagosome formation (41,42). Similar to the kidney proximal tubular cell defect, we observed an increased p62 signal in Vps34^{cKO} thyroids at P14. Accumulation of p62 and LC3b in Vps34^{cKO} indicates a block in the autophagy process. In addition, p62 accumulation also suggests activation of the antioxidant NRF2 pathway by competitive binding of p62 to KEAP1 (33, 43). We indeed observed increased expression of two NRF2 target genes, namely the quinone reductase, *Nqo1*, and the thioredoxin reductase 1, *Txnrd1*. Considering the expected key role of Vps34 in macroautophagy, our data on mitophagy do not prove, but are compatible with the suggestion that this important homeostatic process is abrogated upon Vps34 deficiency.

A final observation deserving discussion is the occurrence of viable cells in the follicular lumens of Vps34^{cKO} thyroids. Our first hypothesis was that defective endocytic and autophagic routes to the lysosomes could impact thyrocyte homeostasis, thus causing

cellular stress. Cellular stress, induced by defective autophagosome and lysosomal function, or by activation of stress kinase such as JNK, could explain shedding of thyrocytes into the colloidal space. However, luminal cells of $Vps34^{cKO}$ thyroids were negative for E-cadherin and the thyrocyte-specific transcription factor TTF-1 (NKX2.1). Furthermore, lineage tracing experiments demonstrated that these luminal cells had never expressed Pax8 and thus did not derive from thyrocytes. The second hypothesis was that the cellular stress and loss of tissue homeostasis would recruit macrophages. Indeed, we found that luminal cells were labelled for the conventional macrophage marker F4/80, are proliferating and display a high LAMP-1 signal. In addition, Tg and I-Tg colocalized with the LAMP-1 structures. This observation contributes to explaining the colloid exhaustion observed in $Vps34^{cKO}$ mice and could thus be responsible for the low levels of circulating T_4. Although the signal(s) attracting macrophages to the colloid is(are) unknown, the loss of tight junction integrity might facilitate their invasion.

Acknowledgements

This work was supported by grants from the Fonds pour la Recherche Scientifique (F.R.S-FNRS, # J.0076.18, Belgium), Université catholique de Louvain (Actions de Recherche concertées to CEP, ARC 15/20-065), and Fondation Roi Baudouin. SR and X-HL were supported by a grant DK15070 from the National Institutes of Health, USA. Work in the laboratory of BV was supported by grants from the MRC (G0700755) and BBSRC (BB/I007806/1; BB/M013278/1). The core facility for Imaging Cells and Tissues was also financed by National Lottery, Région bruxelloise, Région wallonne, Université catholique de Louvain and de Duve Institute. The authors thank Prof. C. Ris-Stalpers for iodo-thyroglobulin antibody, Abdelkadder El Kaddouri and Claude Massart for technical help. GG held a fellowship from the Fonds pour la formation à la Recherche dans l'Industrie et l'Agriculture (FRIA, Belgium), TW was postdoctoral researcher supported by UCLouvain, OD is supported by Télévie, VJ by the Cystinosis Research Foundation, CS is a UCLouvain teaching assistant, HGC was a postdoctoral researcher and CEP is a Senior Research Associate at F.R.S-FNRS.

Author disclosures and contributions

BV is a consultant for Karus Therapeutics (Oxford, UK), iOnctura (Geneva, Switzerland) and Venthera (Palo Alto, US) and has received speaker fees from Gilead. The other authors have no competing financial interest. GG and TSW performed the initial morphological and molecular studies and analyzed the data. OD and CS performed all the other experiments and prepared the figures for the revision. VJ and AS participated in data collection and analysis. HGC was involved in supervision of GG. BB and BV provided the Vps34 mice, XHL and SR assayed T_4 and TSH levels, and CM provided expertise with ^{125}I experiments. PJC and CEP conceived, designed and supervised the project, and wrote the manuscript. All authors have approved the final version of the manuscript.

Name and address of corresponding author

Prof. Christophe E. Pierreux

Cell Biology Unit

de Duve Institute and Université Catholique de Louvain

75, Avenue Hippocrate

B-1200 Brussels

Belgium

Email: christophe.pierreux@uclouvain.be

Thyroid
Vps34 PI 3-kinase controls thyroid hormone production by regulating thyroglobulin iodination, lysosomal proteolysis and tissue homeostasis (DOI: 10.1089/thy.2019.0182)

References

1. Colin IM, Denef JF, Lengele B, Many MC, Gerard AC 2013 Recent insights into the cell biology of thyroid angiofollicular units. Endocr Rev 34:209-238.

2. Carvalho DP, Dupuy C 2017 Thyroid hormone biosynthesis and release. Mol Cell Endocrinol 458:6-15.

3. Cangul H, Liao X-H, Schoenmakers E, Kero J, Barone S, Srichomkwun P, Iwayama H, Serra EG, Saglam H, Eren E, Tarim O, Nicholas AK, Zvetkova I, Anderson CA, Karet Frankl FE, Boelaert K, Ojaniemi M, Jääskeläinen J, Patyra K, Löf C, Williams ED, UK10K Consortium, Soleimani M, Barrett T, Maher ER, Chatterjee VK, Refetoff S, Schoenmakers N 2018 Homozygous loss-of-function mutations in SLC26A7 cause goitrous congenital hypothyroidism. J Clin Ivest Insight 3:e99631.

4. Koumarianou P, Gomez-Lopez G, Santisteban P 2017 Pax8 controls thyroid follicular polarity through cadherin-16. J Cell Sci 130:219-231.

5. Shivas JM, Morrison HA, Bilder D, Skop AR 2010 Polarity and endocytosis: reciprocal regulation. Trends Cell Biol 20:445-452.

6. Rodriguez-Boulan E, Macara IG 2014 Organization and execution of the epithelial polarity programme. Nat Rev Mol Cell Biol 15:225-242.

7. Morrison HA, Dionne H, Rusten TE, Brech A, Fisher WW, Pfeiffer BD, Celniker SE, Stenmark H, Bilder D 2008 Regulation of early endosomal entry by the Drosophila tumor suppressors Rabenosyn and Vps45. Mol Biol Cell 19:4167-4176.

8. Bilanges B, Posor Y, Vanhaesebroeck B 2019 PI3K isoforms in cell signaling and vesicle trafficking. Nat Rev Mol Cell Biol May 20. doi: 10.1038/s41580-019-0129-z. [Epub ahead of print].

9. Lindmo K, Stenmark H 2006 Regulation of membrane traffic by phosphoinositide 3-kinases. J Cell Sci 119:605-614.

10. Juhasz G, Hill JH, Yan Y,Sass M, Baehrecke EH, Backer JM, Neufeld TP 2008 The class III PI(3)K Vps34 promotes autophagy and endocytosis but not TOR signaling in Drosophila. J Cell Biol 181:655-666.

11. Backer JM 2008 The regulation and function of Class III PI3Ks: novel roles for Vps34. Biochem J 410:1-17.

12. Jaber N, Zong WX 2013 Class III PI3K Vps34: essential roles in autophagy, endocytosis, and heart and liver function. Ann NY Acad Sci 1280:48-51.

13. Bechtel W, Helmstädter M, Balica J, Hartleben B, Kiefer B, Hrnjic F, Schell C, Kretz O, Liu S, Geist F, Kerjaschki D, Walz G, Huber TB 2013 Vps34 deficiency reveals the importance of endocytosis for podocyte homeostasis. J Am Soc Nephrol 24:727-743.

14. O'Farrell F, Lobert VH, Sneeggen M, Jain A, Katheder NS, Wenzel EM, Schultz SW, Tan KW, Brech A, Stenmark H, Rusten TE 2017 Class III phosphatidylinositol-3-OH kinase controls epithelial integrity through endosomal LKB1 regulation. Nat Cell Biol 19:1412-1423.

15. Ronan B, Flamand O, Vescovi L, Dureuil C, Durand L, Fassy F, Bachelot M-F, Lamberton A, Mathieu M, Bertrand T, Marquette J-P, El-Ahmad Y, Filoche-Romme B, Schio L, Garcia-Echeverria C, Goulaouic H, Pasquier B 2014 A highly potent and selective Vps34 inhibitor alters vesicle trafficking and autophagy. Nat Chem Biol 10:1013-1019.

16. Nascimbeni AC, Codogno P, Morel E 2017 Phosphatidylinositol-3-phosphate in the regulation of autophagy membrane dynamics. FEBS J 284:1267-1278.

17. Dupont N, Nascimbeni AC, Morel E, Codogno P 2017 Molecular Mechanisms of Noncanonical Autophagy. Intl Rev Cell Mol Biol 328:1-23.

Thyroid
Vps34 PI 3-kinase controls thyroid hormone production by regulating thyroglobulin iodination, lysosomal proteolysis and tissue homeostasis (DOI: 10.1089/thy.2019.0182)
This paper has been peer-reviewed and accepted for publication, but has yet to undergo copyediting and proof correction. The final published version may differ from this proof.

18. Carpentier S, N'Kuli F, Grieco G, Van Der Smissen P, Janssens V, Emonard H, Bilanges B, Vanhaesebroeck B, Gaide Chevronnay HP, Pierreux CE, Tyteca D, Courtoy PJ 2013 ClassIII phosphoinositide 3-kinase/VPS34 and dynamin are critical for apical endocytic recycling. Traffic 14:933-948.

19. Grieco G, Janssens V, Gaide Chevronnay HP, N'Kuli F, Van Der Smissen P, Wang TS, Shan J, Vainio S, Bilanges B, Jouret F, Vanhaesebroeck B, Pierreux CE, Courtoy PJ 2018 Suppression of Vps34 PI 3-kinase activity in kidney proximal tubules abrogates apical trafficking and causes a Fanconi syndrome. Sci Rep 8:14133.

20. Shan J, Jokela T, Skovorodkin I, Vainio S 2010 Mapping of the fate of cell lineages generated from cells that express the Wnt4 gene by time-lapse during kidney development. Differentiation 79:57-64.

21. Bouchard M, Souabni A, Busslinger M 2004 Tissue-specific expression of cre recombinase from the Pax8 locus. Genesis 38:105-109.

22. Valet C, Levade M, Chicanne G, Bilanges B, Cabou C, Viaud J, Gratacap MP, Gaits-Iacovoni F, Vanhaesebroeck B, Payrastre B, Severin S 2017 A dual role for the class III PI3K, Vps34, in platelet production and thrombus growth. Blood 130:2032-2042.

23. Pohlenz J, Maqueem A, Cua K, Weiss RE, Van Sande J, Refetoff S 1999 Improved radioimmunoassay for measurement of mouse thyrotropin in serum: strain differences in thyrotropin concentration and thyrotroph sensitivity to thyroid hormone. Thyroid 9:1265-1271.

24. Delmarcelle AS, Villacorte M, Hick AC, Pierreux CE 2014 An ex vivo culture system to study thyroid development. J Vis Exp 6:88.

25. Hick AC, Delmarcelle AS, Bouquet M, Klotz S, Copetti T, Forez C, Van Der Smissen P, Sonveaux P, Collet JF, Feron O, Courtoy PJ, Pierreux CE 2013 Reciprocal epithelial:endothelial paracrine interactions during thyroid development govern follicular organization and C-cells differentiation. Dev Biol 381:227-240.

Thyroid
Vps34 PI 3-kinase controls thyroid hormone production by regulating thyroglobulin iodination, lysosomal proteolysis and tissue homeostasis (DOI: 10.1089/thy.2019.0182)

Thyroid

Vps34 PI 3-kinase controls thyroid hormone production by regulating thyroglobulin iodination, lysosomal proteolysis and tissue homeostasis (DOI: 10.1089/thy.2019.0182)

26. Dupasquier S, Delmarcelle AS, Marbaix E, Cosyns JP, Courtoy PJ, Pierreux CE 2014 Validation of housekeeping gene and impact on normalized gene expression in clear cell renal cell carcinoma: critical reassessment of YBX3/ZONAB/CSDA expression. BMC Mol Biol 15:9.

27. Massart C, Hoste C, Virion A, Ruf J, Dumont JE, Van Sande J 2011 Cell biology of H2O2 generation in the thyroid: investigation of the control of dual oxidases (DUOX) activity in intact ex vivo thyroid tissue and cell lines. Mol Cell Endocrinol 343:32-44.

28. Zhou X, Takatoh J, Wang F 2011 The mammalian class 3 PI3K (PIK3C3) is required for early embryogenesis and cell proliferation. PloS one 6:e16358.

29. Chen J, Chen MX, Fogo AB, Harris RC, Chen JK 2013 mVps34 deletion in podocytes causes glomerulosclerosis by disrupting intracellular vesicle trafficking. J Am Soc Nephrol. 24:198-207.

30. Bechtel, W, Helmstädter M, Balica J, Hartleben B, Schell C, Huber TB 2013 The class III phosphatidylinositol 3-kinase PIK3C3/VPS34 regulates endocytosis and autophagosome-autolysosome formation in podocytes. Autophagy 9:1097-1099.

31. Cohen-Kaplan V, Ciechanover A, Livneh I 2016 p62 at the crossroad of the ubiquitin-proteasome system and autophagy. Oncotarget 7:83833-83834.

32. Bjorkoy G, Lamark T, Pankiv S, Overvatn A, Brech A, Johansen T 2009 Monitoring autophagic degradation of p62/SQSTM1. Methods Enzymol 452:181-197.

33. Ziros PG, Habeso IG, Chartoumpekis DV, Ntalampyra E, Somm E, Renaud CO, Bongiovanni M, Trougakos IP, Yamamoto M, Kensler TW, Santisteban P, Carrascao N, Ris-Stalpers C, Amendola E, Liao XH, Rossich L, Thomasz L, Juvenal GJ, Refetoff S, Sykiotos GP 2018 NFE2-related transcription factor 2 coordinates antioxidant defense with thyroglobulin production and iodination in the thyroid gland. Thyroid 28:780-798.

34. Grasberger H, De Deken X, Mayo OB, Raad H, Weiss M, Liao XH, Refetoff S 2012 Mice deficient in dual oxidase maturation factors are severely hypothyroid. Mol Endocrinol 26:481-492.

35. Christophe-Hobertus C, Christophe D 2010 Delimitation and functional characterization of the bidirectional THOX-DUOXA promoter regions in thyrocytes. Mol Cell Endocrinol 317:161-167.

36. Twyffels L, Strickaert A, Virreira M, Massart C, Van Sande J, Wauquier C, Beauwens R, Dumont JE, Galietta LJ, Boom A, Kruys V 2014 Anoctamin-1/TMEME16A is the major apical iodide channel of the thyrocyte. Am J Physiol Cell Physiol 307:1102-1112.

37. Jaber N, Mohd-Naim N, Wang Z, DeLeon JL, Kim S, Zhong H, Sheshadri N, Dou Z, Edinger AL, Du G, Braga VM, Zong WX 2016 Vps34 regulates Rab7 and late endocytic trafficking through recruitment of the GTPase-activating protein Armus. J Cell Sci 129:4424-4435.

38. Gaide Chevronnay HP, Janssens V, Van Der Smissen P, Liao XH, Abid Y, Nevo N, Antignac C, Refetoff S, Cherqui S, Pierreux CE, Courtoy PJ 2015 A mouse model suggests two mechanisms for thyroid alterations in infantile cystinosis: decreased thyroglobulin synthesis due to endoplasmic reticulum stress/unfolded protein response and impaired lysosomal processing. Endocrinology 156:2349-2364.

39. Gahl WA, Thoene JG, Schneider JA 2002 Cystinosis. N Engl J Med. 347:111–121.

40. Cherqui S, Courtoy PJ 2017 The renal Fanconi syndrome in cystinosis: pathogenic insights and therapeutic perspectives. Nat Rev Nephr 13:115-131.

41. Hong Z, Pedersen NM, Wang L, Torgersen ML, Stenmark H, Raiborg C 2017 PtdIns3P controls mTORC1 signaling through lysosomal positioning. J Cell Biol 216:4217-4233.

42. Korolchuk VI, Rubinsztein DC 2011 Regulation of autophagy by lysosomal positioning. Autophagy 7:927-928.

43. The selective autophagy substrate p62 activates the stress responsive transcription factor Nrf2 through inactivation of Keap1. Komatsu M, Kurokawa H, Waguri S, Taguchi K, Kobayashi A, Ichimura Y, Sou YS, Ueno I, Sakamoto A, Tong KI, Kim M, Nishito Y, Iemura S, Natsume T, Ueno T, Kominami E, Motohashi H, Tanaka K, Yamamoto M. Nat Cell Biol. 2010 Mar;12(3):213-23. doi: 10.1038/ncb2021. Epub 2010 Feb 21. PMID: 20173742.

Thyroid

Vps34 PI 3-kinase controls thyroid hormone production by regulating thyroglobulin iodination, lysosomal proteolysis and tissue homeostasis (DOI: 10.1089/thy.2019.0182)

Figure legends

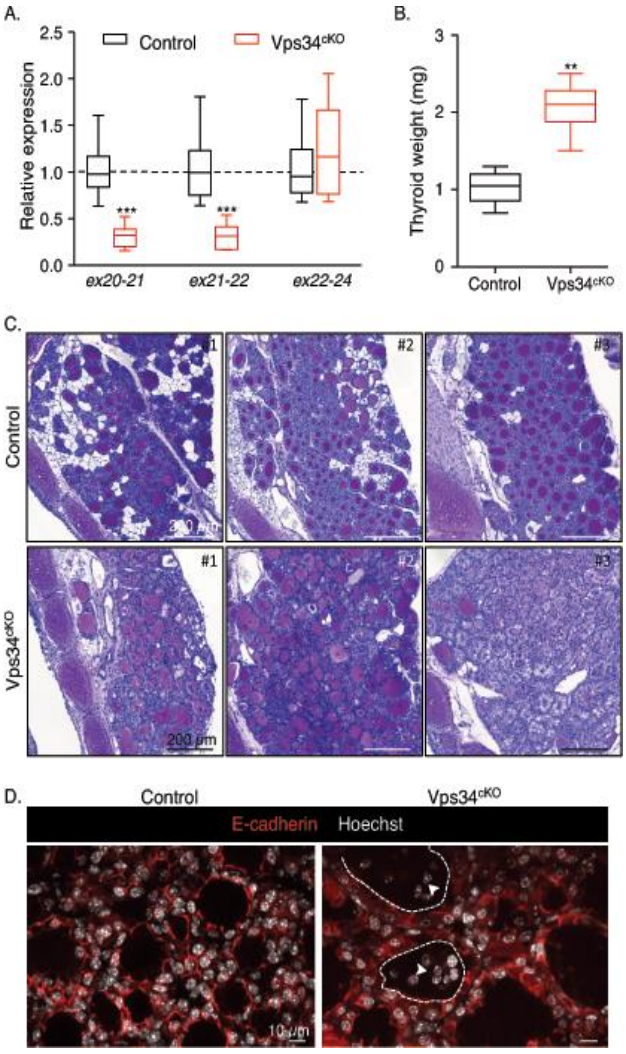

Figure 1. Genetic and histopathological characterization. A. Extensive genetic excision of Vps34 exon 21. Compared with control (black boxes), Vps34^{cKO} thyroid (red boxes) shows ~70% reduction in exon 21 mRNA level at P14. The unchanged mRNA level spanning exons 22-24 serves as control. Boxes with median and percentiles of 10 WT and 11 cKO samples; ***, p< 0.0001 by Mann-Whitney non-parametric test. ***B. Increased thyroid weight.*** Compared with control (black boxes), Vps34^{cKO} thyroid (red boxes) shows a two-fold increase in thyroid weight. Boxes with median and percentiles of 8 WT and 6 cKO samples; **, p< 0.01 by Mann-Whitney non-parametric test. ***C. Histopathological evidence for colloid exhaustion.*** As compared to control thyroid tissues (n=3) where all follicles show regular lumen filling with homogenous and intense PAS (Periodic Acid Shiff) staining, Vps34^{cKO} thyroids (n=3) present fewer, mostly centrally located, PAS-stained follicles and with

weaker staining intensity, other follicles that appear empty (for further quantification, see Supplementary Figure 1). ***D. Vps34^{cKO} thyrocytes are altered and follicles contains abundant non-epithelial cells.*** Nuclei are labeled by Hoechst (shown in white); thyrocyte basolateral contours are labeled for E-cadherin (red); two lumen boundaries are delineated by broken lines. As compared to control thyroid follicles, Vps34^{cKO} follicular structures are frequently irregular and containing additional cells inside the lumen (arrowheads). These cells are not labeled for E-cadherin.

Thyroid
Vps34 PI 3-kinase controls thyroid hormone production by regulating thyroglobulin iodination, lysosomal proteolysis and tissue homeostasis (DOI: 10.1089/thy.2019.0182)
This paper has been peer-reviewed and accepted for publication, but has yet to undergo copyediting and proof correction. The final published version may differ from this proof.

Thyroid

Vps34 PI 3-kinase controls thyroid hormone production by regulating thyroglobulin iodination, lysosomal proteolysis and tissue homeostasis (DOI: 10.1089/thy.2019.0182)

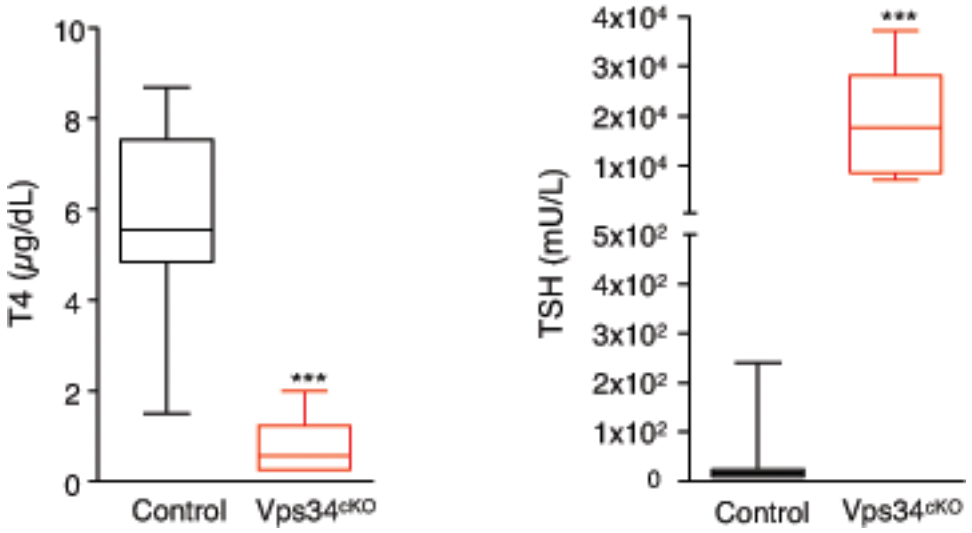

Figure 2. Vps34^{cKO} mice display severe hypothyroidism associated with high TSH levels. As compared to control mice (black boxes), T_4 plasma level in Vps34^{cKO} is extremely low (red boxes). Conversely, TSH levels are dramatically elevated. (10 WT and 9 cKO samples; ***, p= 0.0003 by Mann-Whitney non-parametric test).

Thyroid
Vps34 PI 3-kinase controls thyroid hormone production by regulating thyroglobulin iodination, lysosomal proteolysis and tissue homeostasis (DOI: 10.1089/thy.2019.0182)

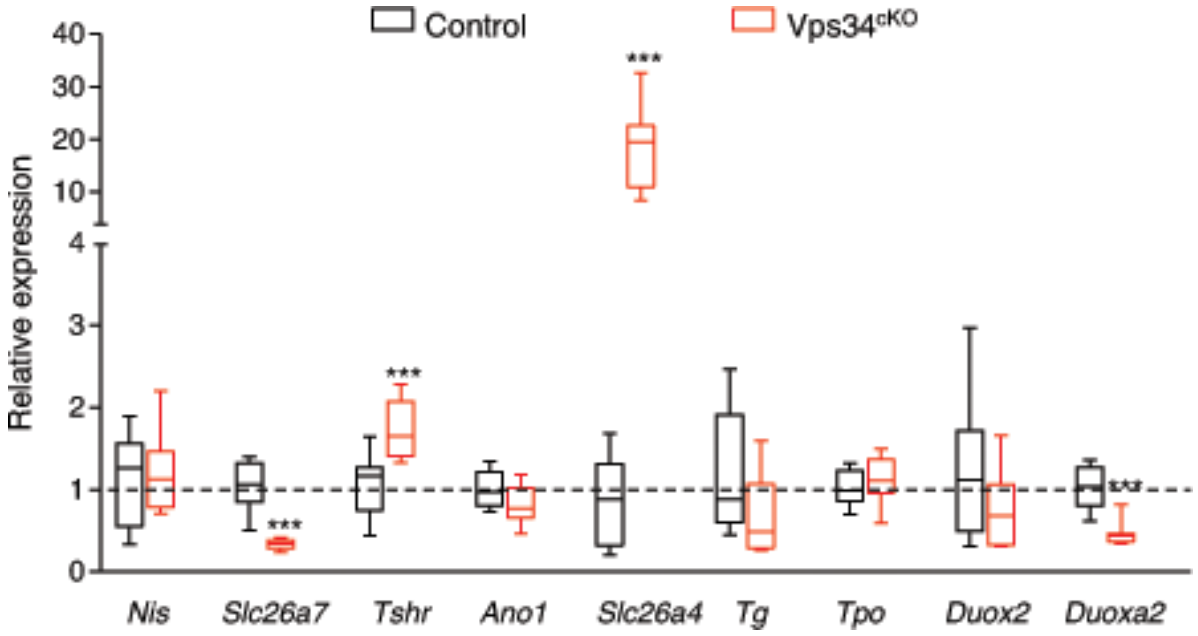

Figure 3. Relative expression level of main actors of thyroid hormonogenesis at P14. Gene expression analysis by RT-qPCR, presented as boxes with median and percentiles. As compared to control thyroid (black boxes), expression in Vps34^{cKO} (red boxes) is preserved for the thyroid-specific genes *Nis*, *Tpo*, *Tg* and *Duox2.* Expression of the TSH receptor (*Tshr*) and of *Slc26a4* is significantly increased in Vps34^{cKO}, while expression of *Slc26a7* and *Duoxa2* is significantly decreased. Boxes with median and percentiles of at least 9 control and 9 Vps34^{cKO} samples; ***, $p < 0.001$ by Mann-Whitney non-parametric test.

Thyroid

Vps34 PI 3-kinase controls thyroid hormone production by regulating thyroglobulin iodination, lysosomal proteolysis and tissue homeostasis (DOI: 10.1089/thy.2019.0182)

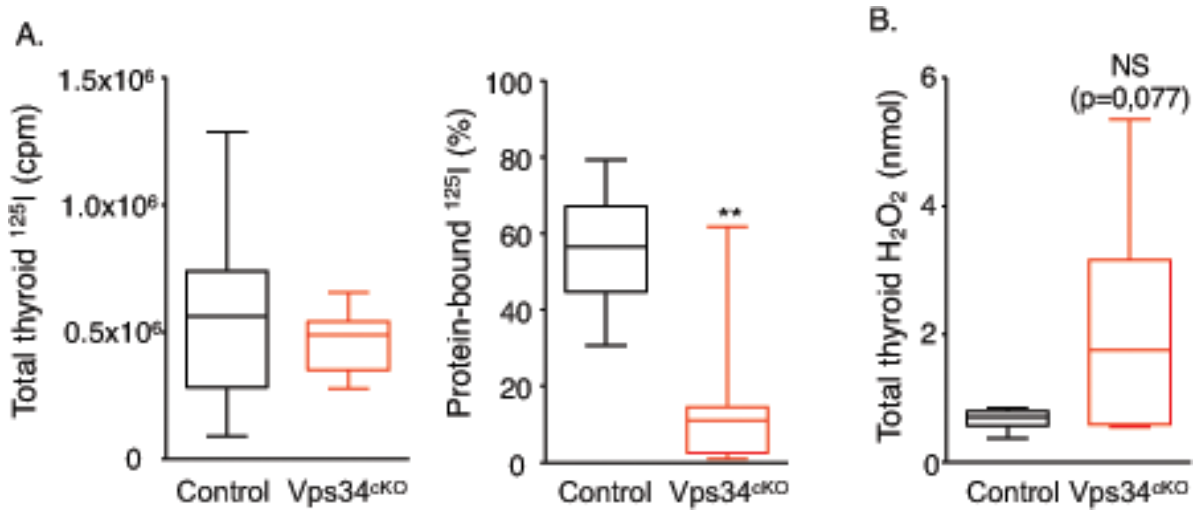

Figure 4. Normal uptake of iodine but major defect of organification in Vps34^{cKO} thyroid.

A. Comparable ^{125}I-iodine uptake in the thyroid in control genotypes (black box) and Vps34^{cKO} thyroid (red box), but much reduced ^{125}I bound to protein (in %) in Vps34^{cKO} thyroid, suggesting defective organification. Boxes with median and percentiles of 39 (10 Flox/+, 19 Flox/Flox, 10 Cre;Flox/+) and 12 Vps34^{cKO} (Cre;Flox/Flox) samples; ***, p< 0.001 by Mann-Whitney non-parametric test. **B**. Level of H_2O_2 in total thyroid extracts show a trend to an increase in Vps34^{cKO} thyroid. Boxes with median and percentiles of 9 control and 9 Vps34^{cKO} samples; p= 0.077 by Mann-Whitney non-parametric test.

Thyroid
Vps34 PI 3-kinase controls thyroid hormone production by regulating thyroglobulin iodination, lysosomal proteolysis and tissue homeostasis (DOI: 10.1089/thy.2019.0182)
This paper has been peer-reviewed and accepted for publication, but has yet to undergo copyediting and proof correction. The final published version may differ from this proof.

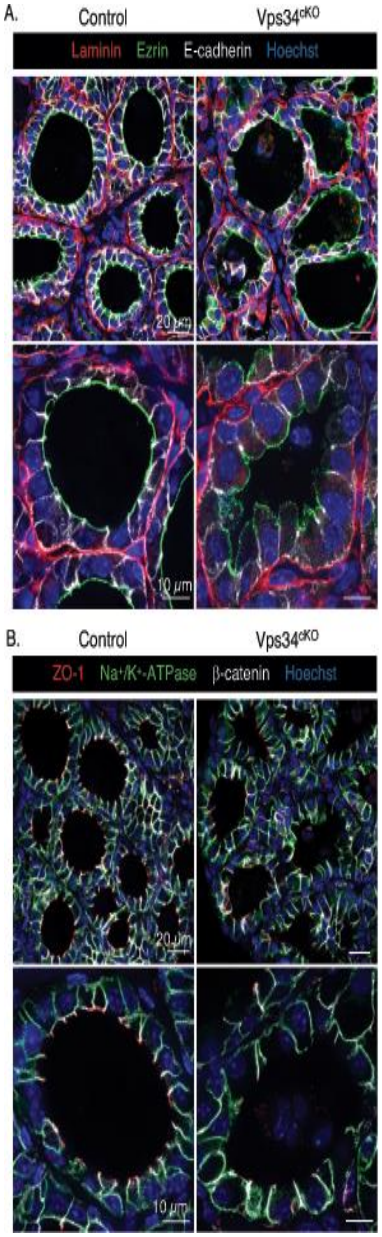

Figure 5. Normal basolateral but impaired apical organization of tyrocytes. A. Thyroid sections from control (left) and Vps34^{cKO} (right) labeled for laminin (red), ezrin (green) and E-cadherin (white). Nuclei are labeled by Hoechst (shown in blue). In control thyroid, laminin surrounds follicles composed of thyrocytes delineated by basolateral E-cadherin and apical ezrin. In Vps34^{cKO}, laminin normally surrounds follicles composed of thyrocytes with well-defined basolateral E-cadherin but weaker and less regular apical ezrin. Note here apical membrane bulging in the colloidal space. ***B.*** Thyroid sections from control (left) and Vps34^{cKO} (right) labeled for ZO-1 (red), Na^+/K^+-ATPase (green) or β-catenin (white). Nuclei are labeled by Hoechst (shown in blue). In control and Vps34^{cKO} thyroid, Na^+/K^+-

ATPase and β-catenin are correctly localized and restricted to the basolateral pole of the thyrocytes, indicating the presence of a tight junction. However, the tight junction-associated protein ZO-1 is only detected at few apico/basolateral junctions.

Thyroid
Vps34 PI 3-kinase controls thyroid hormone production by regulating thyroglobulin iodination, lysosomal proteolysis and tissue homeostasis (DOI: 10.1089/thy.2019.0182)

Thyroid
Vps34 PI 3-kinase controls thyroid hormone production by regulating thyroglobulin iodination, lysosomal proteolysis and tissue homeostasis (DOI: 10.1089/thy.2019.0182)

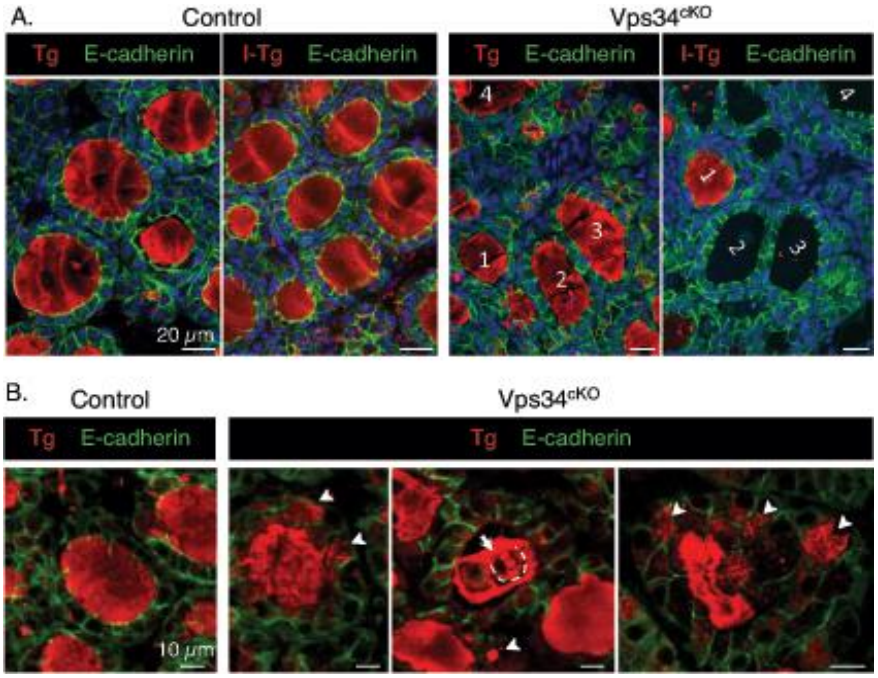

Figure 6. Evidence for defective iodide organification in Vps34^{cKO} thyroid: follicular lumina with Tg but devoid of iodinated-Tg. **A.** Thyroid sections from control (left) and Vps34^{cKO} (right) labeled for E-cadherin (green) and thyroglobulin (red), recognized either for a core protein epitope (Tg), or a hormonogenic peptide (I-Tg). Control follicular lumina are round and uniformly labeled for both Tg and I-Tg. In Vps34^{cKO}, follicular structures are less regular, with the majority containing Tg, but not the hormonogenic peptide. In Vps34^{cKO}, two serial (tilted) sections are shown. ***B. Comparison of Tg labelling in control and Vps34^{cKO} thyrocytes.*** In control follicles, Tg is essentially restricted to lumen, with little or no signal inside thyrocytes. In Vps34^{cKO}, Tg is readily detected within thyrocytes as collections of submicrometric dots or larger spheres (arrowheads). Of note, some luminal cells (broken line in middle panel) also contain Tg-labeled spheres, indicating active endocytosis (arrow).

Thyroid

Vps34 PI 3-kinase controls thyroid hormone production by regulating thyroglobulin iodination, lysosomal proteolysis and tissue homeostasis (DOI: 10.1089/thy.2019.0182)

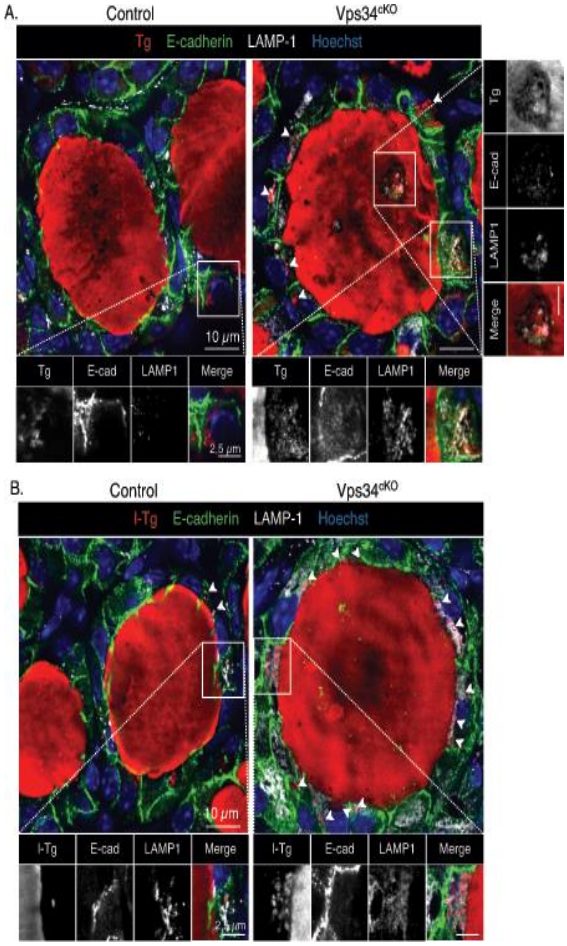

Figure 7. Vps34^{cKO} thyrocytes display increased LAMP-1 signal and impaired I-Tg proteolytic processing. **A.** Thyroid sections from control (left) and Vps34^{cKO} (right) labeled for thyroglobulin (red), E-cadherin (green) and lysosomal LAMP-1 (white). Nuclei are labeled by Hoechst (shown in blue). In control, thyrocytes rarely contain intracellular Tg and LAMP-1 signal is weak. In Vps34^{cKO}, most thyrocytes have intracellular Tg (arrowheads) and LAMP-1 signal is much increased. Insets show magnification with separate emissions, then merged, channels. Note colocalization of Tg with LAMP-1 in luminal cells (at right). **B.** Thyroid sections from control (left) and Vps34^{cKO} (right) labeled for iodinated-thyroglobulin (I-Tg, red), E-cadherin (green) and lysosomal LAMP-1 (white). Nuclei are labeled by Hoechst (shown in blue). As compared to control follicles which show a weak signal for LAMP-1, and rare intracellular I-Tg, LAMP-1 signal is intense in Vps34^{cKO} thyrocytes and intracellular I-Tg dots are frequently observed (arrowheads). As shown in the enlargements below, LAMP-1-labeled structures in Vps34^{cKO} thyrocytes are enlarged or vacuolated as compared to control.

Thyroid
Vps34 PI 3-kinase controls thyroid hormone production by regulating thyroglobulin iodination, lysosomal proteolysis and tissue homeostasis (DOI: 10.1089/thy.2019.0182)

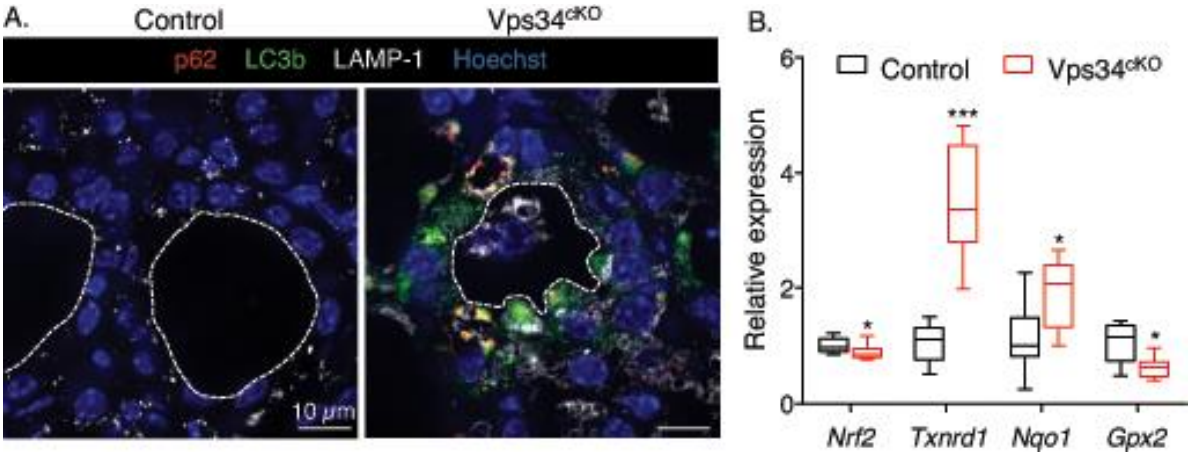

Figure 8. Vps34^{cKO} thyrocytes show strong accumulation of p62 and LC3b dots. **A.** Thyroid sections from control (left) and Vps34^{cKO} (right) labeled for p62 (red), LC3b (green) and lysosomal LAMP-1 (white). Nuclei are labeled by Hoechst (shown in blue). Compared with control follicles, which show low LAMP-1 and almost no signal for p62 and LC3b, all three markers are very strong in Vps34^{cKO} thyroid sections. p62 perfectly co-localizes with LC3b and labels large aggregates. These aggregates are adjacent to LAMP-1-positive structures. **B. Increased NRF2 signaling.** Gene expression analysis by RT-qPCR, presented as boxes with median and percentiles. As compared to control thyroid (black boxes), expression of *Nrf2* is reduced in Vps34^{cKO} (red boxes), but level of two out of three NRF2 target genes, *Txnrd1* and *Nqo1* is increased. Boxes with median and percentiles of at least 9 control and 9 Vps34^{cKO} samples; *, p< 0.05 and ***, p< 0,001 by Mann-Whitney non-parametric test.

Thyroid

Vps34 PI 3-kinase controls thyroid hormone production by regulating thyroglobulin iodination, lysosomal proteolysis and tissue homeostasis (DOI: 10.1089/thy.2019.0182)

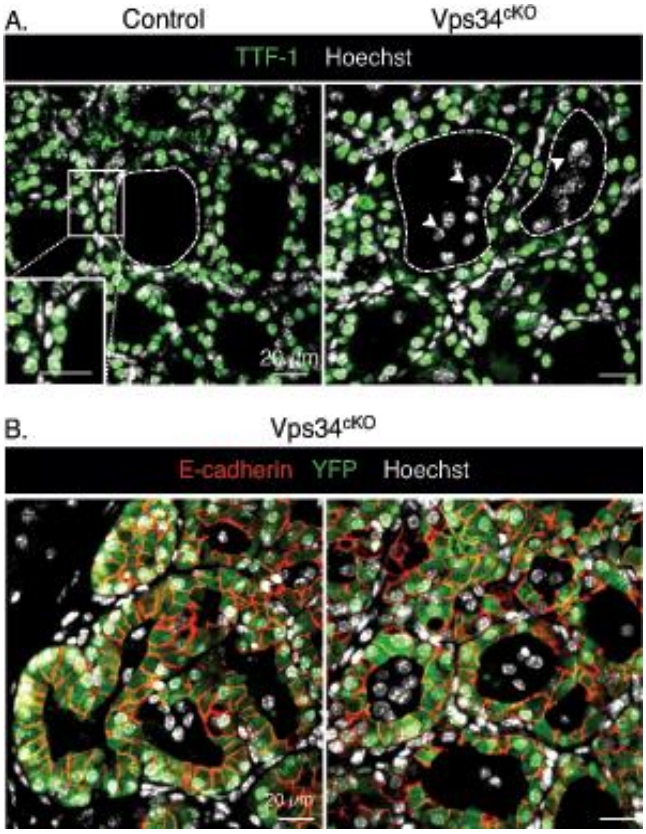

Figure 9. Luminal cells in Vps34^{cKO} thyroid are not thyrocytes*. *A. Immunolabelling for thyrocyte transcription factor-1 (TTF-1, green); nuclei are visualized with the Hoechst stain (shown in white). In both control and Vps34^{cKO} thyroid, nuclei of thyrocytes circumscribing the follicular lumina are all labeled by the thyrocyte-specific transcription-factor-1, TTF-1. As indicated by the arrowheads, nuclei of luminal cells show no signal for TTF-1 (only white signal representing Hoechst). ***B.*** Immunolabelling for E-cadherin (red) and YFP (green); nuclei are visualized with the Hoechst stain (shown in blue). Representative images of Vps34cKO thyroid sections reveal expression of YFP only in cells surrounding the follicular lumina, i.e. in cells where Pax8-Cre has been active. Luminal cells do not derive from thyrocyte progenitors as they are negative for YFP.

Thyroid
Vps34 PI 3-kinase controls thyroid hormone production by regulating thyroglobulin iodination, lysosomal proteolysis and tissue homeostasis (DOI: 10.1089/thy.2019.0182)

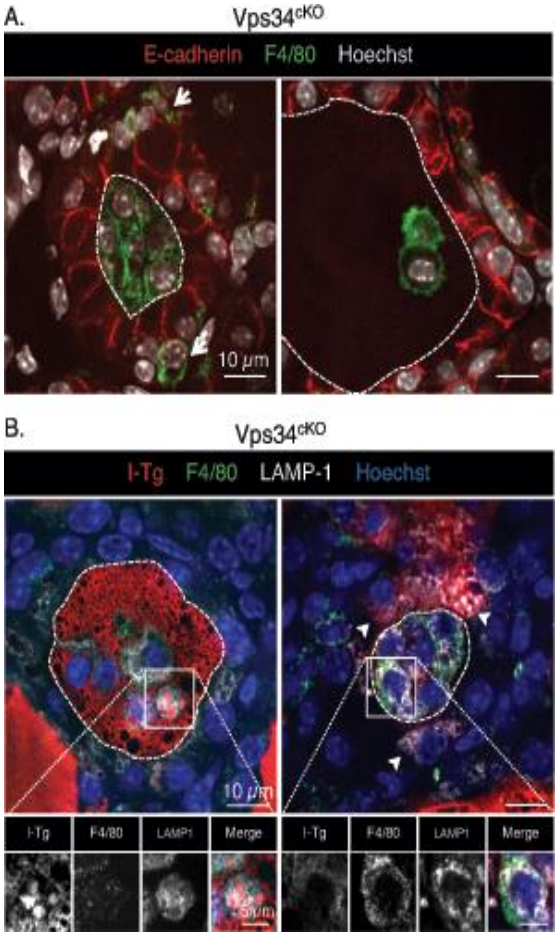

Figure 10. Luminal cells in Vps34^{cKO} thyroid are macrophages. A. Immunolabelling for E-cadherin (red), and for the conventional macrophage marker (F4/80, green); nuclei are visualized with the Hoechst stain (shown in white). In Vps34^{cKO} thyroid, F4/80 signal can be found in the interstitium (arrows), but also in the colloidal space, thus identifying luminal cells as infiltrating macrophages. **D. Luminal cells are taking up the colloid.** Immunolabelling for I-Tg (red), F4/80 (green) and LAMP-1 (white). Nuclei are visualized with the Hoechst stain (shown in blue). Luminal cells in Vps34^{cKO} have abundant LAMP-1 structures that surround I-Tg droplets. Arrowheads show additional I-Tg in thyrocytes. Broken lines indicate luminal contours.

Supplementary Table I: Antibodies and use

Antibody	Supplier	Reference	Species	Dilution	Unmasking	Embedding
Act. Casp. 3	Cell signalling	9661	rabbit	1/100	+	Paraffin
β-catenin	BD Biosciences	610154	mouse IgG1	1/1000	+	paraffin
E-Cadherin	BD Biosciences	610182	mouse IgG2a	1/1000	- or +	paraffin or gelatin
Ezrin	Thermo scientific	MS-661-P1	mouse IgG1	1/400	+	paraffin
F4/80	Cell signalling	70076	rabbit	1/250	+	paraffin
I-Thyroglobulin	Gift : Ris Stalpers		mouse IgG1	1/100	+	paraffin
Ki67	BD Biosciences	556003	mouse IgG1	1/250	+	paraffin
Laminin	Sigma	L9393	rabbit	1/100	+	paraffin
LAMP-1	Hybridoma Bank	1D4B	rat (Mab)	1/100	-	paraffin or gelatin
LAMP-2A	Abcam	Ab18528	rabbit	1/200	+	paraffin
LC3B	Cell signalling	3868	rabbit	1/100	+	paraffin
Na^+/K^+-ATPase	Hybridoma bank	α6F	mouse IgG2a	1/400	+	paraffin

Thyroid

Vps34 PI 3-kinase controls thyroid hormone production by regulating thyroglobulin iodination, lysosomal proteolysis and tissue homeostasis (DOI: 10.1089/thy.2019.0182)

p62	ARP	03-GP62C	guinea pig	1/400	+	paraffin or gelatin
TOM20	Cell signalling	D8T4N	rabbit	1/200	+	paraffin
Thyroglobulin	DAKO	M0781	mouse IgG1	1/500	+	paraffin
TTF1	Agilent	M357501	mouse IgG1	1/200	+	paraffin
YFP	Abcam	Ab6673	goat	1/250	+	Paraffin or gelatin
ZO-1	Invitrogen	61-7300	rabbit	1/75	+	paraffin

GriecoTable 1

Thyroid
Vps34 PI 3-kinase controls thyroid hormone production by regulating thyroglobulin iodination, lysosomal proteolysis and tissue homeostasis (DOI: 10.1089/thy.2019.0182)
This paper has been peer-reviewed and accepted for publication, but has yet to undergo copyediting and proof correction. The final published version may differ from this proof.

Supplementary Table II: Primers

gene	**forward primer (5' → 3')**	**reverse primer (5' → 3')**
Ano1	*GAGGCCAGTAGCCATCAGAG*	*CGTGAAGGAGATCACAAAGGC*
β-actin	TCCTGAGCGCAAGTACTCTGT	CTGATCCACATCTGCTGGAAG
Duox	TCCAGAAGGCGCTGAACAG	GCGACCAAAGTGGGTGATG
Duoxa2	CGTTAACATTACACTCCGAGGAACA	CAGAATGCCACCCACAGTGT
Gpx2	GCTTCCCTTGCAACCAGTTC	CTCCCCTTCTGGCCCTATGA
Nis	AGCAGGCTTAGCTGTATCCC	AGCCCCGTAGTAGAGATAGGAG
Nqo1	CGTCATTCTCTGGCCGATTCA	GGGGAAAAAGAAAGCTGCGT
Nrf2	GAATTCCTCCCAATTCAGCCG	GCTGCCTCCAGAGAGCTATT
Rpl27	GCCCTGGTGGCTGGAATTGACC	AAACTTGACCTTGGCCTCCCGC
Slc26a4	GCTCGCATTCGGGACTGTAA	CAGCAAACCTGCTTTGGCAT
Slc26a7	CTCAGTTCCCTGTCCAACGG	AGCGTGGAGACTCCTGTGTA
Tg	TGGGACGTGAAAGGGGAATGGTGC	GTGAGCTTTTGGAATGGCAGGCGA
Tpo	TGCCAACAGAAGCATGGGCAAC	GCACAAAGTTCCCATTGTCCAC
Tshr	CTGCGGGGCAAAGAGTGTGC	AGGGGAGCTCTGTCAAGGCA
Txnrd1	TACTGCATCAGCAGTGATGATC	CCATGTTCTTCCATGTGTTCAC
Vps34 ex20-21	CACACAGTATCCAGCACAGC	TGAGACTGGACCCTATGGCA
Vps34 ex21-22	TTGGAGTTGGAGACCGGCA	TCCTTGTTCAGCTTCATCGGAG
Vps34 ex22-24	GATGGTGGAAGGGATGGGTG	CGCTCTCGTCGATCAGACTC

GriecoTable 2

Thyroid
Vps34 PI 3-kinase controls thyroid hormone production by regulating thyroglobulin iodination, lysosomal proteolysis and tissue homeostasis (DOI: 10.1089/thy.2019.0182)

Thyroid
Vps34 PI 3-kinase controls thyroid hormone production by regulating thyroglobulin iodination, lysosomal proteolysis and tissue homeostasis (DOI: 10.1089/thy.2019.0182)

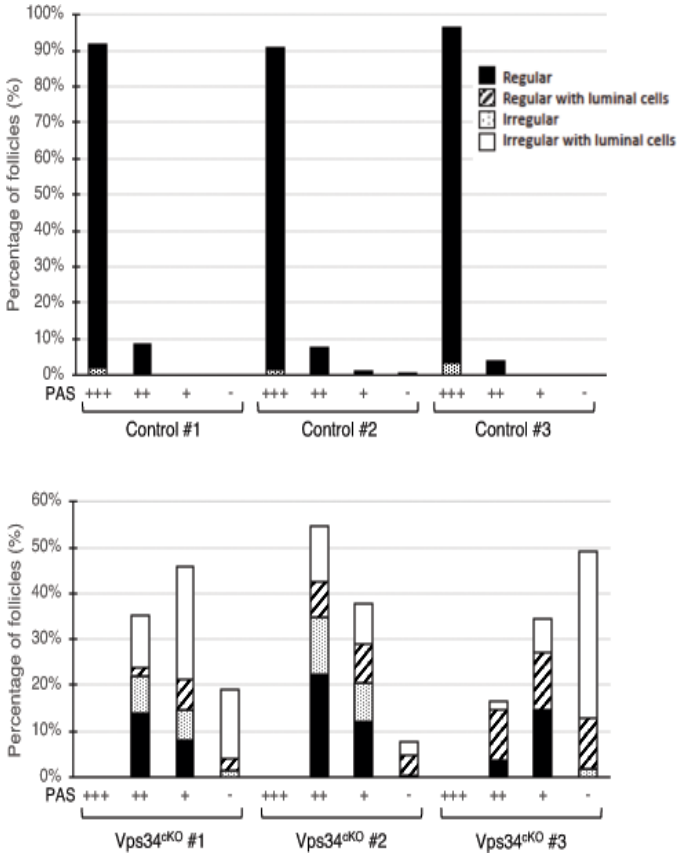

***Suppl Fig. 1. Histopathological evidence of colloid exhaustion*: quantification.** Follicles from three controls and three Vps34^{cKO} sections stained with PAS were classified in four groups: regular follicle (black), regular follicle with luminal cells (dashed), irregular follicle (dotted) and irregular with luminal cells (white). In addition, each follicle group was assigned a PAS intensity: stronger than cartilage (PAS+++), similar to cartilage (PAS++), weaker than cartilage (PAS+) and no PAS staining (PAS-). In control, most follicles are regular and PAS++. In Vps34^{cKO}, the four type of follicles can be found and most follicles have low (PAS+) or no PAS staining.

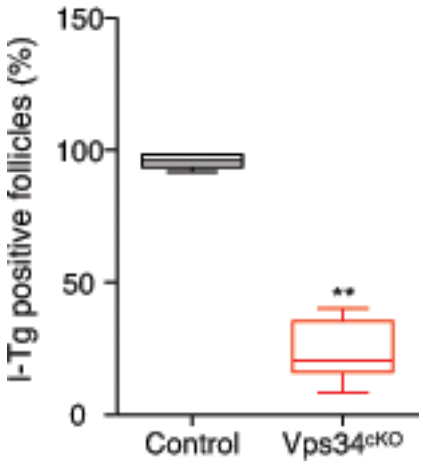

***Suppl Fig. 2. Histopathological evidence of I-Tg defect*: quantification.** Follicles from five controls and seven Vps34^{cKO} sections stained with I-Tg were counted for the presence of the T_4 hormonogenic peptide. Results are expressed as a percentage of I-Tg positive follicles (2712 control follicles and 3436 Vps34^{cKO} were counted). As compared to control mice (black box; 96 ± 2,68 %), only a quarter (red box; 25 ± 11,93 %) of Vps34^{cKO} follicles were positive for I-Tg (**, p= 0.01 by Mann-Whitney non-parametric test).

Thyroid
Vps34 PI 3-kinase controls thyroid hormone production by regulating thyroglobulin iodination, lysosomal proteolysis and tissue homeostasis (DOI: 10.1089/thy.2019.0182)

Thyroid
Vps34 PI 3-kinase controls thyroid hormone production by regulating thyroglobulin iodination, lysosomal proteolysis and tissue homeostasis (DOI: 10.1089/thy.2019.0182)

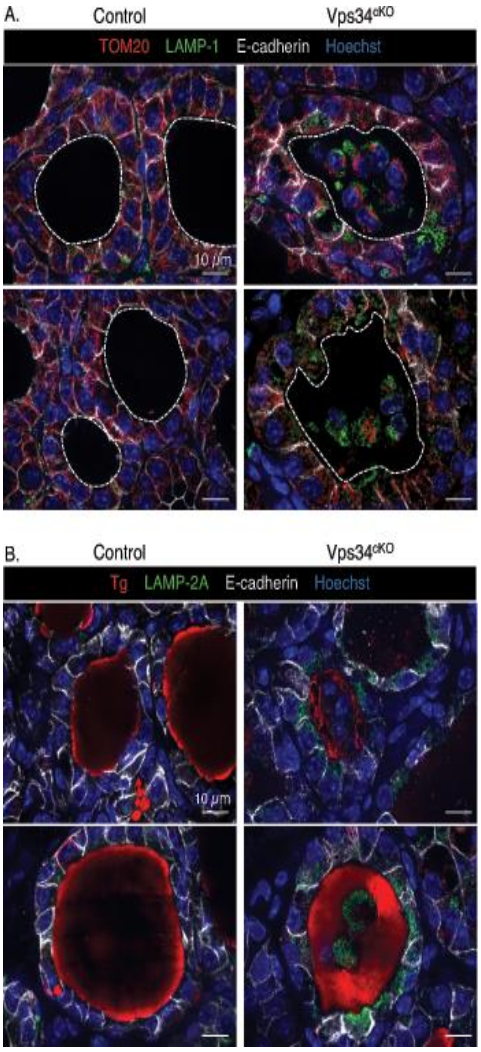

Suppl Fig. 3. Macroautophagy and chaperone-mediated autophagy. A. Thyroid sections from control (left) and Vps34^{cKO} (right) labeled for TOM20 (red), lysosomal LAMP-1 (green) and E-cadherin (white). Nuclei are labeled by Hoechst (presented in blue). In control and Vps34^{cKO}, TOM20 shows a perinuclear localization without co-localization with LAMP-1 (no yellow), even though LAMP-1 signal is more widespread. ***B.*** Thyroid sections from control (left) and Vps34^{cKO} (right) labeled for thyroglobulin (red), LAMP-2A (green) and E-cadherin (white). Nuclei are labeled by Hoechst (shown in blue). In Vps34^{cKO} sections, LAMP-2A signal is much stronger than in control thyroid.